Homochiral growth through enantiomeric cross-inhibition

A. Brandenburg[*], A. C. Andersen, S. Höfner and M. Nilsson

Nordita, Blegdamsvej 17, DK-2100 Copenhagen Ø, Denmark
(∗ author for correspondence, e-mail: brandenb@nordita.dk, phone +45 353 25228, fax: +45 353 89157)

Abstract. The stability and conservation properties of a recently proposed polymerization model are studied. The achiral (racemic) solution is linearly unstable once the relevant control parameter (here the fidelity of the catalyst) exceeds a critical value. The growth rate is calculated for different fidelity parameters and cross-inhibition rates. A chirality parameter is defined and shown to be conserved by the nonlinear terms of the model. Finally, a truncated version of the model is used to derive a set of two ordinary differential equations and it is argued that these equations are more realistic than those used in earlier models of that form.

1. Introduction

The chirality of molecules in living organisms must have been fixed at an early stage in the development of life. All life that we know is based on RNA and DNA molecules with dextrarotatory sugars. There is growing evidence that the RNA world (Woese, 1967; Crick, 1968; Orgel, 1968; see also Wattis & Coveney 1999) must have been preceded by a simpler pre-RNA world made up of achiral constituents (Bada, 1995, Nelson *et al.,* 2000). An alternative carrier of genetic code are peptide nucleic acids or PNA (Nielsen, 1993). These can be rather simple and are currently discussed in connection with the idea to build artificial life (Rasmussen *et al.,* 2003). Furthermore, although PNA can still be chiral (Tedeschi *et al.,* 2002), there are also forms of PNA that are achiral (Pooga *et al.,* 2001), suggesting that chirality may have developed later when the first RNA molecules formed.

In current proposals to build artificial life, chirality does not seem to be crucial. The PNA molecules is proposed to act primarily as charge carrier, i.e. a very primitive functionality compared to the genetic code in contemporary cells (Rasmussen *et al.,* 2003). At this stage, homochirality may have been introduced by chance. This is also supported by the fact that chiral polymers of the same chirality tend to have a more stable structure (Pogodina *et al.,* 2001) and would therefore be genetically preferred.

Since the introduction of chiral molecules is assumed to take place at a stage when there is already growth and self-replication, it is also plausible to assume that the existence of chiral molecules has an auto-catalytic effect in producing new chiral molecules of the same chirality (Kondepudi *et al.*, 1990). This is the basis of the recently proposed polymerization model of Sandars (2003); see also Wattis & Coveney (2004). The purpose of the present paper is to reconsider this model (or a slightly modified version of it) and to analyze its stability behavior and conservation properties. We also discuss and illustrate some of the salient features of the model in more detail. The model is then compared with earlier models of homochirality where the detailed polymerization process is ignored and the dynamics of single variables representing left and right handed polymers are modeled instead (Frank, 1953; Kondepudi and Nelson, 1984; Goldanskii and Kuzmin 1989; Avetisov and Goldanskii, 1993; Saito and Hyuga, 2004).

In order to appreciate the nature of the many terms in the model of Sandars we begin by discussing first the basic principle of the model in connection with homochiral polymer growth and then turn to the full set of reactions that are included in the model.

2. Homochiral polymer growth

In this section we discuss the growth of polymers by adding monomers of the same chirality, i.e. we ignore reactions with monomers of the opposite chirality. This is conceptually the simplest case, but its equilibrium solution also corresponds to a solution of the full system discussed below. We write down the equations for left-handed polymers, but the same applies also to right-handed polymers.

A left-handed polymer of length n is assumed to react with a left-handed monomer via the reaction

$$L_n + L_1 \rightarrow L_{n+1} \quad (n \geq 1). \tag{1}$$
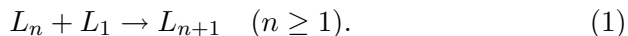
The reaction rate is k_S, but since L_n can bind to L_1 on either side, the total reaction rate is $2k_S$ and proportional to the product of the concentrations of the two constituents. We denote the concentration of L_n chains by $[L_n]$, so in a volume V the number of L_n chains is $N_n \equiv [L_n]V$. For $n \geq 3$ the number of possible pairs of L_{n-1} and L_1 is $N_n \times N_1$. A special situation arises for $n = 2$, because then L_1 is interacting with another L_1, and the number of possible pairs is only $\frac{1}{2}N_1(N_1 - 1) \approx \frac{1}{2}N_1^2$. [This problem is familiar from the physics of nuclear reactions; see, e.g., Kippenhahn and Weigert (1990).] We

therefore introduce the factor $\sigma_n^{(1/2)}$ defined by

$$\sigma_n^{(\alpha)} = \begin{cases} \alpha & \text{for} \quad n = 2, \\ 1 & \text{for} \quad n \geq 3. \end{cases} \tag{2}$$

(Later we shall use this factor also with $\alpha = 0$ instead of 1/2.) The corresponding contribution to the evolution of the concentration of L_n is therefore

$$\frac{\mathrm{d}[L_{n+1}]}{\mathrm{d}t} = \dots + 2k_S\sigma_n^{(1/2)}[L_n][L_1], \tag{3}$$

where the dots denote the presence of other terms that will be discussed later.

Obviously, the concentrations of L_n and L_1 have to decrease at the same rate by the same amount, so

$$\frac{\mathrm{d}[L_n]}{\mathrm{d}t} = \dots - 2k_S\sigma_n^{(1/2)}[L_n][L_1], \tag{4}$$

$$\frac{\mathrm{d}[L_1]}{\mathrm{d}t} = \dots - 2k_S\sigma_n^{(1/2)}[L_{n-1}][L_1]. \tag{5}$$

In the following we regard n as a general index with $2 \leq n \leq N$, the evolution of $[L_n]$ is governed by the difference of two terms (gain from L_{n-1} chains and loss in favor of producing L_{n+1} chains). The production of each L_n contributes to a loss of L_1 monomers, so the right hand side of Eq. (5) becomes a sum over all n. The full set of equations is then

$$\frac{\mathrm{d}[L_1]}{\mathrm{d}t} = Q_L - \lambda_L[L_1], \quad \text{where} \quad \lambda_L = 2k_S\sum_{n=1}^{N-1}[L_n], \tag{6}$$

$$\frac{\mathrm{d}[L_n]}{\mathrm{d}t} = 2k_S[L_1]\left(\sigma_n^{(1/2)}[L_{n-1}] - [L_n]\right), \tag{7}$$

where Q_L denotes the production of new L_1 monomers (see below). A corresponding set of equations applies also to right-handed polymers, i.e. R_1 and R_n. Note that Eqs. (6) and (7) obey the conservation law

$$\frac{\mathrm{d}E_L}{\mathrm{d}t} = Q_L - 2k_S[L_1][L_N], \tag{8}$$

where

$$E_L = \sum_{n=1}^{N} n[L_n] \tag{9}$$

is the total number of left-handed building blocks. This number reaches an equilibrium if the supply of new left-handed monomers, Q_L, balances the loss associated with reactions involving the longest polymers possible for a given value of N.

Equation (7) shows that in the steady state we have $[L_n] = \frac{1}{2}[L_1]$ for all $n \geq 2$. Using Eq. (6), we find $\lambda_L = k_S N[L_1]$, and therefore

$$2[L_n] = [L_1] = \sqrt{Q_L/k_S N} \quad \text{(steady state)} \tag{10}$$

is a possible equilibrium solution.

New left and right handed monomers are assumed to be continuously reproduced from an achiral (racemic) substrate. The rates of regeneration, Q_L and Q_R, depend on the concentration of the substrate, $[S]$, and in some fashion on the relative concentrations of right and left handed polymers. So, in general, we write

$$Q_L = k_C[S]\left\{\frac{1}{2}(1+f)C_L + \frac{1}{2}(1-f)C_R + C_{0L}\right\}, \tag{11}$$

$$Q_R = k_C[S]\left\{\frac{1}{2}(1+f)C_R + \frac{1}{2}(1-f)C_L + C_{0R}\right\}, \tag{12}$$

where C_L and C_R are some measures of the catalytic effect of the already existing right and left handed polymers, and the terms C_{0L} and C_{0R} allow for the possibility of non-catalytic production of left and right handed monomers – possibly at different rates. (Unless noted otherwise, we keep $C_{0L} = C_{0R} = 0$.)

The concentration of the substrate is assumed to be maintained by a source Q, so we have

$$\frac{\mathrm{d}[S]}{\mathrm{d}t} = Q - (Q_L + Q_R), \tag{13}$$

where $Q_L + Q_R = k_C[S](C_L + C_R + C_{0L} + C_{0R})$; see Eqs. (11) and (12). In general, we expect C_L and C_R to be some function of L_n and R_n, respectively. Sandars (2003) assumed $C_L = [L_N]$ and $C_R = [R_N]$, i.e. the catalytic effect depends on the concentrations of the longest possible chains of left and right handed polymers. This assumption imposes a dependence on the cutoff value N, a dependence that should preferably be avoided in numerical or other technical considerations. The model should for example be stable and consistent in the limit when N is infinite. Another option would be to assume $C_L = [L_M]$ and $C_R = [R_M]$, where $M < N$ is a fixed value that is independent of the maximum chain length. Both alternatives have the disadvantage that $[L_1]$ and $[R_1]$ can never grow unless $[L_M]$ or $[R_M]$ are initially also finite. While it is plausible that long chains carry more catalytic weight than shorter ones, the dependence of the results on the particular choice of M seems artificial. (The allowance of finite values of C_{0L} and C_{0R} would remove this problem, although in practice both of these values should still be quite small.)

On may expect that the catalytic properties of the existing left and right handed polymers depend on the length of the polymer. The exact functional expression for this dependence is not known. It is therefore important that a model that explains homochirality is not sensitive to the details of the catalytic properties and hence the functional form of C_L and C_R. It turns out that the qualitative behavior of the model of Sandars is indeed robust in this respect, e.g. a pitchfork bifurcation exists in both Sandars' original and in our model. To avoid artificial dependence on the maximal chain length N, we chose to let the catalytic functions have the following form

$$C_L = E_L, \quad C_R = E_R, \tag{14}$$

where E_L is given by Eq. (9), and E_R is defined analogously. This is similar to the choice of Wattis & Coveney (2004) who assumed, independently of us, $C_L = E_L - [L_1]$ and $C_R = E_R - [R_1]$.

We now comment on another aspect of the model of Sandars. He assumed that in the evolution of $[L_N]$ the loss is not $2k_S[L_1][L_N]$, as it would be if Eq. (7) were applied to $n = N$, but he introduced an explicit linear damping term instead. This implies that the model behaves discontinuously at the end of the chain. We feel that an "extrapolating" (continuous) behavior is more reasonable, so we choose to apply Eq. (7) also at $n = N$.

It is interesting to note that in the continuous limit, Eq. (7) becomes

$$\left(\frac{\partial}{\partial t} + 2k_S[L_1]\frac{\partial}{\partial n} \right) [L_n] = 0, \tag{15}$$

which describes waves traveling toward larger n. This is shown in Figure 1, where we have perturbed the equilibrium solution (10) by a gaussian and have solved Eqs. (6)–(7) numerically. The wave is damped and has a speed that is proportional to $(k_S Q)^{1/2}$, because for the steady state background solution $[L_1] \sim (k_S/Q)^{1/2}$. Note that the extrapolating boundary condition at $n = N$ allows the wave to escape freely.

In this paper we do not adopt the nondimensionalization of Sandars. Instead, we note that there are only two physical dimensions in this problem: time and volume. Characteristic quantities with the dimensions of time and volume are $(k_S Q)^{-1/2}$ and $(k_S/Q)^{1/2}$, respectively. We therefore present all results by explicitly quoting these dimensions. In practice this means that from now on we use $Q = k_S = 1$ as numerical values, but we keep the symbols in the equations for clarity. Throughout this paper we also assume $k_C/k_S = 1$; calculations with different values do not seem to affect our results in any important way.
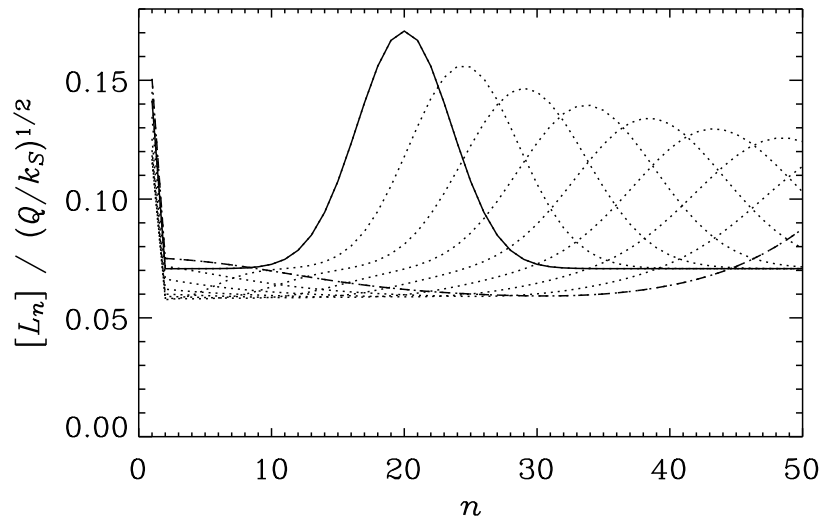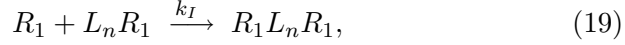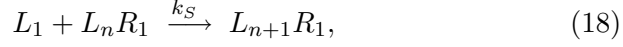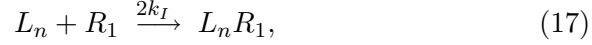
Figure 1. Wave-like propagation of a finite amplitude perturbation. The initial pro-
file is a gaussian. Note the undisturbed propagation of the wave out of the chain at
$n = N$. The time difference between the different curves is $20/(k_S Q)^{1/2}$. We have
shown the first and last times as solid and dashed lines, and all other times as dotted
lines. The parameters are $N = 50$ and $k_C/k_S = 1$.

The fact that the equilibrium solution is constant for all $n \geq 2$
implies that this value will decrease for longer choices of N. In that
sense the solution is never converged. This situation changes when
we allow the ends of the left-handed polymers to be spoiled by right-
handed monomers, as done by Sandars (2003). This will be discussed
in the next section.

3. Enantiomeric cross-inhibition

Already 20 years ago, Joyce *et al.,* (1984) showed in an important
paper describing experiments with template-directed polymerization
that, once a monomer of the opposite chirality is bound to one end
of the chain, the polymerization terminates on that end of the chain.
Sandars (2003) incorporated this effect in his model and showed that
this can lead to a bifurcation into two possible solutions of opposite
chirality and hence to homochirality.

The full set of reactions included in his model is (for $n \geq 2$)

$$L_n + L_1 \xrightarrow{2k_S} L_{n+1}, \tag{16}$$

$$L_n + R_1 \xrightarrow{2k_I} L_nR_1, \tag{17}$$

$$L_1 + L_nR_1 \xrightarrow{k_S} L_{n+1}R_1, \tag{18}$$

$$R_1 + L_nR_1 \xrightarrow{k_I} R_1L_nR_1, \tag{19}$$

and for all four equations we have the complementary reactions obtained by exchanging $L \rightleftarrows R$. Following Sandars (2003), we have introduced the new parameter k_I, which quantifies that rate of enantiomeric cross-inhibition. The special case $k_I = 0$ corresponds to the case discussed in the previous section.

The most important effect of enantiomeric cross-inhibition is that a certain fraction of chains becomes spoiled by producing L_nR_1 and R_nL_1 polymers. Equation (7) and its complementary equation for right-handed polymers suffer therefore a loss proportional to $2k_I$, so we have instead

$$\frac{d[L_n]}{dt} = 2k_S[L_1]\left(\sigma_n^{(1/2)}[L_{n-1}] - [L_n]\right) - 2k_I[L_n][R_1], \tag{20}$$

$$\frac{d[R_n]}{dt} = 2k_S[R_1]\left(\sigma_n^{(1/2)}[R_{n-1}] - [R_n]\right) - 2k_I[R_n][L_1]. \tag{21}$$

These equations allow us to see what happens in the racemic case with $[R_n] = [L_n]$. In a steady state we have (for $n \geq 2$)

$$[L_n] = \tfrac{1}{2}a^{-(n-1)}[L_1] \quad \text{(racemic solution)}, \tag{22}$$

where we have defined $a = 1 + k_I/k_S$. In particular, if $k_I = k_S$, then $[L_n] = 2^{-n}[L_1]$, i.e. $[L_n]$ drops by a factor of 2 from one n to the next, except for $n = 1$ to 2, where it drops by a factor of 4. We should note, however, that this solution can be unstable (see Section 4).

So far, we have not yet considered the evolution equations for the concentrations of the mixed terms, L_nR_1 and R_nL_1. Following Sandars (2003), we abbreviate the corresponding concentrations by $[L_nR]$ and $[R_nL]$, respectively, i.e. without the subscript 1 on the terminating end of the chain. The effect of generating these terms was already manifested in Eqs. (20) and (21) through the appearance of the last term proportional to $2k_I$. Nevertheless, we do need to solve for $[L_nR]$ and $[R_nL]$ explicitly, because the reactions (18) and (19) consume L_1 and R_1 monomers, respectively. The evolution equations for $[L_1]$ and $[R_1]$ are therefore given by

$$\frac{d[L_1]}{dt} = Q_L - \lambda_L[L_1], \quad \frac{d[R_1]}{dt} = Q_R - \lambda_R[R_1], \tag{23}$$

where

$$\lambda_L = 2k_S \sum_{n=1}^{N-1} [L_n] + 2k_I \sum_{n=1}^{N} [R_n] + k_S \sum_{n=2}^{N-1} [L_n R] + k_I \sum_{n=2}^{N} [R_n L], \quad (24)$$

$$\lambda_R = 2k_S \sum_{n=1}^{N-1} [R_n] + 2k_I \sum_{n=1}^{N} [L_n] + k_S \sum_{n=2}^{N-1} [R_n L] + k_I \sum_{n=2}^{N} [L_n R], \quad (25)$$

are the decay rates that quantify the losses associated with the reactions (16)–(19), respectively.

In Eqs. (24) and (25) the concentrations $[L_n R]$ and $[R_n L]$ enter, so we have to solve their corresponding evolution equations (for $n \geq 2$)

$$\frac{\mathrm{d}[L_n R]}{\mathrm{d}t} = k_S [L_1]\Big(\sigma_n^{(0)}[L_{n-1}R] - [L_n R]\Big) + k_I [R_1]\Big(2[L_n] - [L_n R]\Big), \quad (26)$$

$$\frac{\mathrm{d}[R_n L]}{\mathrm{d}t} = k_S [R_1]\Big(\sigma_n^{(0)}[R_{n-1}L] - [R_n L]\Big) + k_I [L_1]\Big(2[R_n] - [R_n L]\Big), \quad (27)$$

where the $\sigma_n^{(0)}$ factor turns off the first term for $n = 2$; see Eq. (2). In Eqs. (26) and (27) the first two terms proportional to k_S correspond to the homochiral growth on the unspoiled end, i.e. reaction (18). The third term comes from reaction (17) and the fourth term comes from reaction (19) and enters here and also in Eqs. (24) and (25) as a loss term. For completeness, we note that the corresponding gain enters in the evolution equations

$$\frac{\mathrm{d}[RL_n R]}{\mathrm{d}t} = k_I [R_1][L_n R], \quad \frac{\mathrm{d}[LR_n L]}{\mathrm{d}t} = k_I [L_1][R_n L], \quad (28)$$

which are not explicitly required for constructing a solution, because these polymers no longer react with the monomers. Nevertheless, solving Eq. (28) simultaneously with Eqs. (20) and (21) and Eqs. (23)–(27) can be useful for monitoring the evolution of the net chirality; see Section 5.

Note that, in contrast to the equations given by Sandars (2003), the truncation levels for the terms $[L_n]$, $[L_n R]$, and $[RL_n R]$ are here the same, i.e. $n \leq N$ for both terms, whereas in the model of Sandars the longest $L_n R_1$ chain has $n = N - 1$, and the longest $R_1 L_n R_1$ chain has only $n = N - 2$. The reason we need to keep the same truncation levels for all three types of polymers is that we want to ensure that the behavior near the end of the chain ($n = N$) does not deviate from the behavior elsewhere ($n < N$); see the discussion in Section 2. For example, to ensure continuous behavior of $[L_n]$ at $n = N$ we need to keep the term $-2k_I[L_N][R_1]$ in Eq. (20). This term, however, is the loss resulting from the gain of $[L_N R]$, so we have to keep the evolution
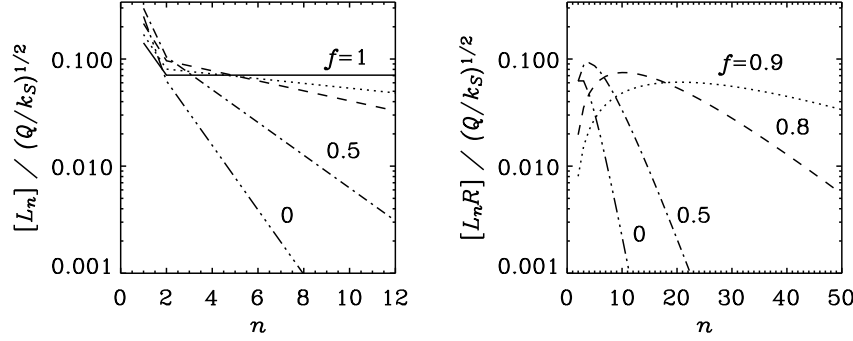
Figure 2. $[L_n]$ (left) and $[L_nR]$ (right) of equilibrium solutions for different values of f. For $f = 1$ we have $[L_nR] = 0$, which cannot be seen in the logarithmic representation.

equation for this term as well. Furthermore, the evolution equation for this term involves, in turn, the term $-k_I[R_1][L_NR]$, which is the loss corresponding to the gain of $[RL_NR]$. If one regards the truncation level N as an unrealistic feature of the model, as we do, then all three polymer types should be truncated at the same level.

In Figure 2 we show $[L_n]$ and $[L_nR]$ for a number of equilibrium solutions for different values of f and $k_I/k_S = 1$. The corresponding values of $[R_n]$ and $[R_nL]$ are small and not shown, except when $f = 0$ in which case the solution is fully racemic with $[R_n] = [L_n]$ and $[R_nL] = [L_nR]$ and is simply

$$[L_nR] = (n - 1)[L_n] = (n - 1)2^{-n}[L_1]. \tag{29}$$

For $f = 1$ the solution is given by Eq. (10).

For $k_I/k_S = 0.1$ the results are similar to those for $k_I/k_S = 1$ provided $f > 0.8$. For $f < 0.7$, however, the solution is fully racemic and therefore the curves are independent of f. This racemic solution is similar to the case $k_I/k_S = 1$ and $f = 0.8$ that is shown in Figure 2.

4. Stability of the racemic equilibrium

A realistic model of homochirality must also have an achiral (racemic) equilibrium solution. It is generally anticipated that this racemic solution can be destabilized in the presence of catalytic reactions (Frank, 1953; Avetisov and Goldanskii, 1993). If the probabilities of adding left and right handed monomers to a homochiral polymer are equal, i.e.
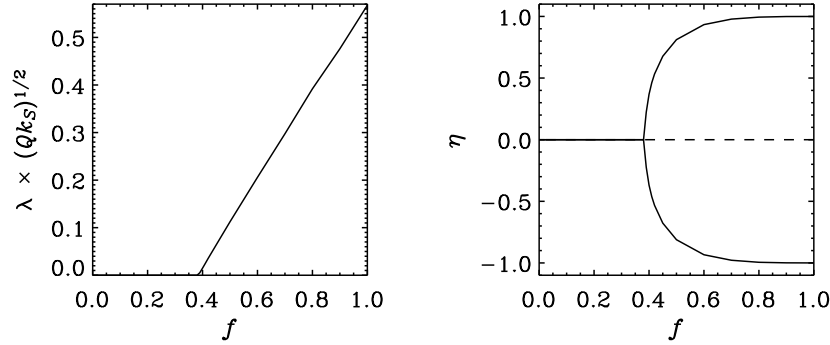
Figure 3. Growth rate (left) and bifurcation diagram showing a classical pitchfork bifurcation (right) as a function of fidelity for $k_I/k_S = 1$, and $N = 50$. The dashed line indicates an unstable solution.

if $k_I = k_S$, the racemic solution given by Eq. (29) is also a possible solution for other values of the fidelity than $f = 0$, but it may of course be unstable.

We have carried out a numerical stability analysis by adding a small (10^{-5}) relative perturbation to the value of $[L_1]$ of the racemic solution. It turns out that for certain values of the fidelity f the departure of $[L_1]$ from the racemic equilibrium solution, $\delta[L_1]$, growth exponentially in time like $e^{\lambda t}$. In Figs 3 and 4 we plot λ obtained from the slope of the graph of $\ln \delta[L_1](t)$ during the exponential growth phase, i.e. before a new nonlinear equilibrium is attained. In Figs 3 and 4 we also plot the corresponding chiral polarization parameter, η, as a function of f. Here we have chosen to define η as

$$\eta = (E_R - E_L) / (E_R + E_L). \tag{30}$$

It turns out that for $k_I/k_S = 1$ the racemic solution is unstable when $f > 0.39$, and for $k_I/k_S = 0.1$ it is unstable when $f > 0.735$. The transition from an achiral to a chiral solution is a typical example of a pitchfork bifurcation; see Figs 3 and 4. This result is in qualitative agreement with Sandars (2003) who found that for $k_I/k_S = 1$ the critical value of f is around 0.21. The differences in the numerical values are explained by differences in the model (e.g., the coupling to the substrate and the length of the maximum polymer length).

The growth rate of the instability is important for determining the time it takes for an almost racemic solution to become homochiral (or at least non-racemic for $f \neq 1$). When $k_I/k_S = 1$, the growth rate λ is around 0.5, but it becomes significantly smaller when the value of k_I
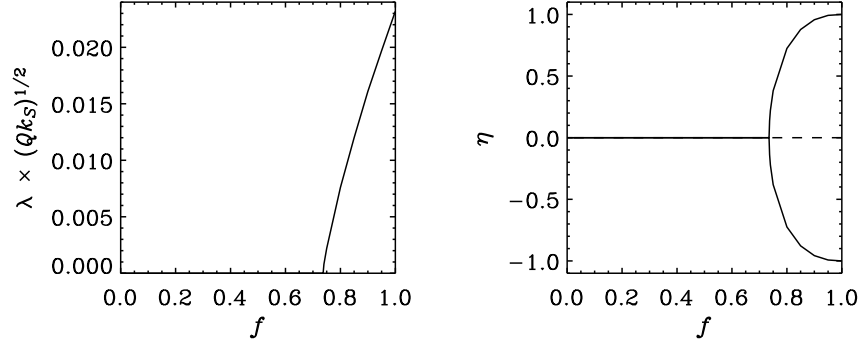
Figure 4. Same as Figure 3, but for $k_I/k_S = 0.1$.

is reduced. This shows explicitly that homochirality emerges as being due to enantiomeric cross-inhibition.

5. Conservation of chirality

For homochiral growth the relevant conservation law is given by Eq. (8) for E_L, and similarly for E_R. In general, however, because of the interaction with left and right handed monomers, there are no longer separate conservation laws for E_L and E_R. Instead, the complete set of equations, Eqs. (20) and (21) together with Eqs. (23)–(25), satisfies

$$\frac{\mathrm{d}}{\mathrm{d}t}\Delta\tilde{E} = \Delta Q - \Delta\Lambda, \qquad (31)$$

where $\Delta Q = Q_R - Q_L$ and $\Delta\Lambda = \Lambda_R - \Lambda_L$ are the net input and output rates of chirality, respectively, and $\Delta\tilde{E} = \tilde{E}_R - \tilde{E}_L$ is the total chirality, where

$$\tilde{E}_R = \sum_{n=1}^{N} n[R_n] + \sum_{n=2}^{N}(n-1)[R_nL] + \sum_{n=3}^{N}(n-2)[LR_nL], \qquad (32)$$

$$\tilde{E}_L = \sum_{n=1}^{N} n[L_n] + \sum_{n=2}^{N}(n-1)[L_nR] + \sum_{n=3}^{N}(n-2)[RL_nR], \qquad (33)$$

denote the total numbers of right and left handed building blocks (or enantiomers), where opposite enantiomers are counted such that they annihilate enantiomers of the opposite chirality. The loss terms resulting from the finite truncation level, N, are denoted by

$$\Lambda_R = 2k_S N[R_1][R_N] + k_S(N-1)[R_1][R_NL], \qquad (34)$$

$$\Lambda_L = 2k_S N[L_1][L_N] + k_S(N-1)[L_1][L_N R]. \tag{35}$$

In order to evaluate the quantities $\tilde{E}_R$ and $\tilde{E}_L$ we have to integrate the evolution equations (28) for the production of terminally spoiled polymers – even though they undergo no further evolution. In a sense the integration of the terminally spoiled polymers acts only as counters that keeps track of the number of polymers that are lost during the polymerization process.

The expressions for $\tilde{E}_R$ and $\tilde{E}_L$ involve sums over $[LR_nL]$ and $[RL_nR]$, but since these quantities do not occur on the right hand sides of the governing evolution equations, their values are not constrained by the dynamics and depend on the initial conditions and continue to evolve in time even though the system may have reached an equilibrium. The so defined net chirality can therefore not be used to characterize a particular solution, and we have to restrict ourselves either to E_R and E_L, or to $\hat{E}_R$ and $\hat{E}_L$, which are defined by taking only the first two sums in Eqs. (36) and (37), i.e.

$$\hat{E}_R = \sum_{n=1}^{N} n[R_n] + \sum_{n=2}^{N} (n-1)[R_n L], \tag{36}$$

$$\hat{E}_L = \sum_{n=1}^{N} n[L_n] + \sum_{n=2}^{N} (n-1)[L_n R]. \tag{37}$$

In Table I we list the resulting values of η, defined in Eq. (30), an analogously defined $\hat{\eta} = (\hat{E}_R - \hat{E}_L)/(\hat{E}_R + \hat{E}_L)$, $\Delta E = E_R - E_L$, and $\Delta \hat{E} = \hat{E}_R - \hat{E}_L$. We also give the mean polymer lengths, $N_R = \sum n[R_n]/\sum[R_n]$ and $N_L = \sum n[L_n]/\sum[L_n]$, of right and left handed polymers.

6. Comparison with other models

The polymerization model of Sandars (2003) is significantly different from all the previously proposed models of homochirality that ignore the detailed polymerization process by only describing some scalar quantities, say x and y, that are representative of the number of left and right handed polymers. In the papers by Saito and Hyuga (2004) it was shown that neither linear nor nonlinear autocatalytic behavior suffice to produce homochirality, and that a backreaction term is needed. Their model equations are

$$\begin{aligned} \dot{x} &= x^2(1-r) - \epsilon x \\ \dot{y} &= y^2(1-r) - \epsilon y \end{aligned} \quad \text{(SH model)} \tag{38}$$

Table I. Numerical results for η, $\hat{\eta}$, ΔE, and $\Delta \hat{E}$ for different values of f. The $\pm$ indicates that these values can have either sign. The last column gives the typical value of N necessary for obtaining a converged result representing the limit $N \to \infty$. For $f = 1$ the results for ΔE $(= \Delta \hat{E})$ and N_R do not converge and we give the analytic expression for arbitrary N instead.

f	$\pm\eta$	$\pm\hat{\eta}$	$\pm\Delta E$	$\pm\Delta\hat{E}$	N_R	N_L	N
1	1	1	$\frac{1}{4}[N(N+1)+2]/N^{1/2}$	$\frac{1}{2}N+1/(N+1)$	–	N
0.9	0.999	0.9999	30.61	143.73	19.0	1.0	500
0.8	0.995	0.9986	10.28	45.06	9.0	1.1	200
0.7	0.978	0.993	5.170	20.99	5.6	1.1	100
0.6	0.933	0.975	2.949	11.01	3.9	1.2	100
0.5	0.813	0.907	1.648	5.597	2.8	1.2	50
0.4	0.368	0.482	0.491	1.500	1.9	1.5	50
0.38	0	0	0	0	1.7	1.7	20

where $r = x + y$ and ϵ is the feedback parameter. For $\epsilon = 0$ there is a continuous range of solutions along the line $r \equiv x + y = 1$, i.e. homochirality does not emerge unless the initial condition is already homochiral. For finite (but small) values of ϵ there are two nontrivial stable fixed points. (The trivial solution, $x = y = 0$, is always a stable fixed point in this model.)

The model of Saito and Hyuga (2004), hereafter the SH model, does capture the expected behavior, but it remains unsatisfactory in that its functional form has been introduced ad hoc. It is therefore desirable to derive simple model equations based on the polymerization equations of Sandars (2003). It turns out that, without changing the basic properties of the model, a minimal version is still meaningful for $N = 2$, and that the equations for the semi-spoiled polymers, $[L_2R]$ and $[R_2L]$, can be ignored (as already done by Sandars). Thus, we only solve Eqs. (20) and (21) together with Eqs. (23)–(25). Following Sandars (2003), we also assume that $C_L = [L_2]$ and $C_R = [R_2]$ (instead of $C_L = E_L$ and $C_R = E_R$, which would yield more complicated expressions). A further simplification can be made by regarding $[L_2]$ as a rapidly adjusting variable that is enslaved to $[L_1]$ (and similarly for $[R_2]$). This technique is also known as the adiabatic elimination of rapidly adjusting variables (e.g., Haken, 1983). Equation (20) becomes

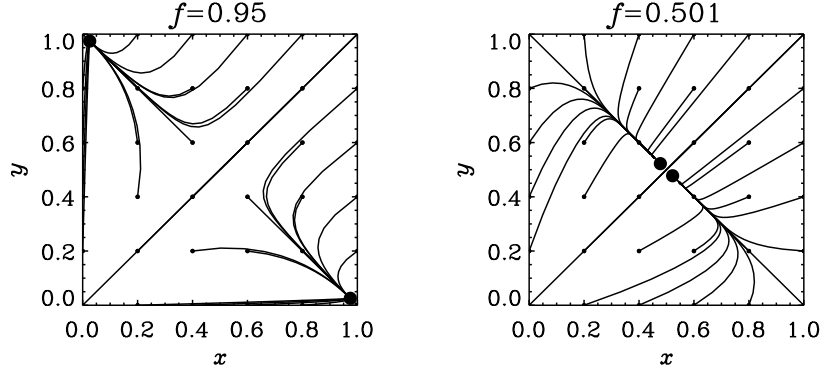$$0 = k_S[L_1]^2 - 2[L_2]\Big(k_S[L_1] + k_I[R_1]\Big), \qquad (39)$$

Figure 5. Phase diagram showing the trajectories of solutions of Eq. (42) for two different values of f. The starting points of each trajectory are marked by small dots and stable fixed points are marked by big dots.

which is solved for $[L_2]$ (and similarly for $[R_2]$), which in turn couples back to the equations for $[L_1]$ and $[R_1]$ via Q_L and Q_R. Finally, we also treat the substrate $[S]$ as a rapidly adjusting variable, i.e. we have $k_C[S] = Q/([L_2] + [R_2])$. We emphasize that the adiabatic elimination does not affect the accuracy of steady solutions. It is convenient to introduce new dimensionless variables,

$$x = [R_1](2k_S/Q)^{1/2}, \quad y = [L_1](2k_S/Q)^{1/2}, \quad \tau = t(Qk_S/2)^{1/2}. \quad (40)$$

In order to compare first with the SH model we restrict ourselves to the special case $k_I/k_S = f = 1$, which leads to the revised model equations

$$\begin{aligned}
\dot{x} &= x^2/\tilde{r}^2 - rx, \\
\dot{y} &= y^2/\tilde{r}^2 - ry,
\end{aligned} \quad (41)$$

where dots denote derivatives with respect to τ and $r = x + y$ and $\tilde{r}^2 = x^2 + y^2$ has been introduced for brevity. Equations (41) resemble the equations of the SH model in that both have a quadratic term proportional to x^2 (or y^2), which is quenched either by a $1 - r$ factor (in the SH model) or by a $1/\tilde{r}^2$ factor in our model. Furthermore, both models have a backreaction term proportional to $-x$ (or $-y$), but the coefficient in front of this term (ϵ in the SH model) is not constant but equal to r.

In the general case with $k_I/k_S \neq 1$, $f \neq 1$, as well as finite values of $C_{0x} = C_{0R}(2k_S/Q)^{1/2}$, and $C_{0y} = C_{0L}(2k_S/Q)^{1/2}$, the equations read

$$\begin{aligned}
\dot{x} &= (p\tilde{x}^2 + q\tilde{y}^2 + C_{0x})/\tilde{r}^2 - r_x x, \\
\dot{y} &= (p\tilde{y}^2 + q\tilde{x}^2 + C_{0y})/\tilde{r}^2 - r_y y,
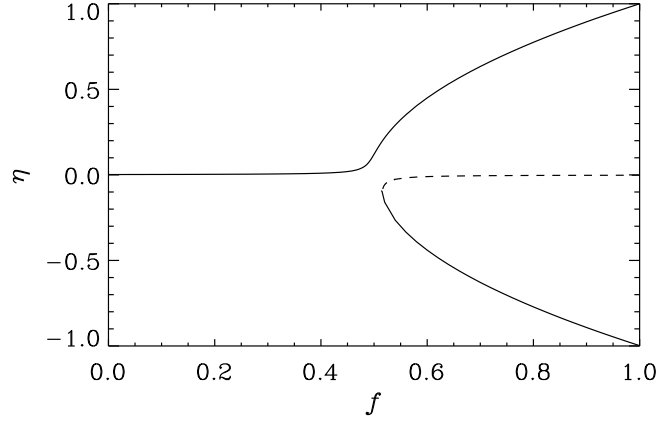\end{aligned} \quad (42)$$

Figure 6. Imperfect bifurcation obtained by solving Eq. (42) for $C_{0x} = 0.001$ and $C_{0y} = 0$ using the Newton-Raphson method.

where we have introduced the abbreviations $r_x = x + y k_I/k_S$, $r_y = y + x k_I/k_S$, $\tilde{x}^2 = x^2/2r_x$, $\tilde{y}^2 = y^2/2r_y$, $\tilde{r}^2 = \tilde{x}^2 + \tilde{y}^2 + C_{0x} + C_{0y}$, $p = (1+f)/2$, and $q = (1-f)/2$.

In Figure 5 we show trajectories of solutions of Eq. (42) for two different values of f in an (x, y) phase diagram. Note that all equilibrium solutions lie on the line $r = 1$. This property allows us to calculate equilibrium solutions for general values of f. Inserting $y = 1 - x$ yields a cubic equation of which one solution is always $x = 1/2$. This reduces the problem to a quadratic equation with the solution

$$x = \tfrac{1}{2} \begin{cases} 1 \pm \sqrt{2f - 1} & \text{for } f \geq 1/2, \\ 1 & \text{otherwise.} \end{cases} \tag{43}$$

Linearizing the equations around the racemic solution, $x = y = 1/2$, yields the growth rate

$$\lambda = 2f - 1. \tag{44}$$

In agreement with our numerical results for large values of N, this equation gives a linear dependence of the growth rate on the fidelity. This result also shows that for $f < 1/2$ perturbations decay exponentially.

In the presence of a biased, non-catalytic generation of monomers (finite C_{0x} or C_{0y} with $C_{0x} \neq C_{0y}$) there is no longer a perfectly racemic equilibrium solution. The sign of η for the solution for $f = 0$ depends on the sign of $C_{0x} - C_{0y}$. Along this solution branch η goes further away from zero in a continuous fashion until $f = 1$. At some value of f a pair of new solutions emerges, one is stable and the other one unstable,

but both have the opposite sign of η; see Figure 6. Among these new branches, the stable one can only be reached via a finite amplitude perturbation. This behavior is called an imperfect bifurcation and has long been anticipated in this context (Kondepudi and Nelson, 1983; Kondepudi *et al.*, 1986; Goldanskii and Kuzmin, 1989).

The steady solutions shown in Figure 6 have been obtained by solving Eq. (42) using the Newton-Raphson method. This method allows us to find both stable and unstable solutions. Near the bifurcation point the diagram is extremely sensitive to the addition of a bias parameter. It is remarkable that for a value as small as $C_{0x} = 10^{-3}$ a relatively large gap has been produced in the bifurcation diagram.

Finite values of C_{0x} and C_{0y} could result from physical influences, for example polarized synchrotron radiation from neutron stars (but see Bonner, 1999), UV radiation in star-forming regions (Bailey, 2001), or the parity violation of the electroweak force (e.g., Hegstrom, 1984). In all these cases the expected effect is however very small (Bada, 1995). We emphasize, however, that the main reason for homochirality is the instability of the racemic (or nearly racemic) solution, which is hardly modified by a finiteness of C_{0x} or C_{0y}.

7. Conclusions

The origin of homochirality has long been thought to be the result of a bifurcation process that can vastly amplify a very small random enantiomeric excess which can then prevail forever. Generic model equations reproducing the expected bifurcation behavior have so far mostly been proposed on an ad hoc basis. It was therefore difficult to establish a connection between model and reality. According to the work of Saito and Hyuga (2004) one expects two effects to be important: nonlinearity and backreaction. However, the functional form of these terms remained open. Furthermore, the meaning of non-perfect catalytic fidelity and enantiomeric cross-inhibition within the framework of the model were not clear. In the present paper we have established a direct connection between the more detailed polymerization model of Sandars (2003) and the simpler model equation approach with only two ordinary differential equations. In particular, the present work has confirmed that the relevant nonlinearity is indeed quadratic (as in the SH model), but it is not quenched like $1-r$, but rather like $1/\tilde{r}^2$, where r and $\tilde{r}$ are measures of the total concentrations of monomers (both right and left handed). Furthermore, the feedback coefficient is not a small constant, as in the SH model, but it is itself proportional to r. More importantly, imperfect fidelity and enantiomeric cross-inhibition,

as well as the effects of a weakly biased non-catalytic production of new monomers, have a quantitative meaning within the framework of the reduced model.

For a more quantitative comparisons of the polymerization process with experiments the full set of equations of Sandars (with the revisions discussed above) is to be preferred. A number of features that can only be captured by the full model. An example is the wave-like propagation in the distribution of homochiral polymers. An experimental confirmation would help to quantify the growth coefficient k_S characterizing the probability that a polymer grows by a monomer of the same chirality. On the other hand, the growth coefficient for enantiomeric cross-inhibition, k_I, determines primarily the minimum fidelity parameter, f, above which bifurcation and hence homochiral growth is at all possible. It is indeed quite remarkable, that the main reason homochiral growth occurs is that binding with a wrong enantiomer spoils further polymerization on the corresponding end of the chain. This leads to competition which is always a key feature of natural selection processes such as these.

Homochirality in living organisms is a singular phenomenon. Non-living chemical systems do in general not have a preferred chirality. In the models presented in this paper this is reflected in Figs 3 and 6. The region of the phase diagram displaying homochirality is characterized by high fidelity, i.e. high auto-catalytic accuracy. The fidelity is expected to be significantly higher in living systems. When an organism dies the auto-catalytic polymerization stops and as a consequence the fidelity is sharply decreased. The characteristic behavior of the polymerization changes from the chiral to the racemic region of the phase diagram. The relaxation of the system from the homochiral to the racemic state is often very slow. It was in fact suggested by Hare and Mitterer (1967) and later by Bada *et al.,* (1970) that racemization of amino acids in fossil material could be used as a dating method. Unfortunately it has turned out that the rate of racemization is strongly temperature dependent, which tends to make this dating method unreliable.

References

Avetisov, V. A. and Goldanskii, V.: 1993, Chirality and the equation of 'biological big bang', *Phys. Lett.* **A 172**, 407–410.

Bada, J. L., Luyendyk, B. P., and Maynard, J. B.: 1970, Marine Sediments: Dating by the Racemization of Amino Acids, *Science* **170**, 730–732.

Bada, J. L.: 1995, Origins of homochirality, *Nature* **374**, 594–595.

Bailey, J.: 2001, Astronomical sources of circularly polarized light and the origin of homochirality, *Orig. Life Evol. Biosph.* **31**, 167–183.

Bonner, W. A.: 1999, Chirality amplification – the accumulation principle revisited, *Orig. Life Evol. Biosph.* **29**, 615–624.

Crick, F. H. C.: 1968, The origin of the genetic code, *J. Mol. Biol.* **38**, 367–379.

Frank, F.: 1953, On Spontaneous Asymmetric Synthesis, Biochim. Biophys. Acta 11, 459-464.

Goldanskii, V. I. and Kuzmin, V. V.: 1989, Spontaneous breaking of mirror symmetry in nature and origin of life, *Sov. Phys. Uspekhi* **32**, 1–29.

Haken, H.: 1983, *Synergetics – An Introduction*, Springer: Berlin.

Hare, P. E. and Mitterer, R. M.: 1967, Nonprotein amino acids in fossil shells, *Yearbook Carnegie Institution of Washington* **65**, 362–364.

Hegstrom, R. A.: 1984, Parity nonconservation and the origin of biological chirality – theoretical calculations, *Orig. Life* **14**, 405–414.

Joyce, G. F., Visser, G. M., van Boeckel, C. A. A., van Boom, J. H., Orgel, L. E., and Westrenen, J.: 1984, Chiral selection in poly(C)-directed synthesis of oligo(G), *Nature* **310**, 602–603.

Kippenhahn, R. and Weigert, A.: 1990, *Stellar structure and evolution*, Springer: Berlin.

Kondepudi, D. K. and Nelson, G. W.: 1983, Chiral symmetry breaking in nonequilibrium chemical systems, *Phys. Rev. Lett.* **50**, 1023–1026.

Kondepudi, D. K. and Nelson, G. W.: 1984, Chiral symmetry breaking in nonequilibrium chemical systems: time scales for chiral selection, *Phys. Lett.* **106A**, 203–206.

Kondepudi, D. K., Moss, F., and McClintock, P. V. E.: 1986, Observation of symmetry breaking, state selection and sensitivity in a noisy electron system, *Physica* **21D**, 296–306.

Kondepudi, D. K., Kaufman, R. J., and Singh, N.: 1990, Chiral symmetry breaking in sodium chlorate crystallization, *Science* **250**, 975–976.

Nelson, K. E., Levy, M., and Miller, S. L.: 2000, Peptide Nucleic Acids rather than RNA may have been the first genetic molecule, *Proc. Nat. Acad. Sci. U.S.A.* **97**, 3868–3871.

Nielsen, P. E.: 1993, Peptide nucleic acid (PNA): A model structure for the primordial genetic material, *Orig. Life Evol. Biosph.* **23**, 323–327.

Orgel, L. E.: 1968, Evolution of the genetic apparatus, *J. Mol. Biol.* **38**, 381–393.

Pogodina, N. V., Lavrenko, V. P., Srinivas, S., and Winter, H. H.: 2001, Rheology and structure of isotactic polypropylene near the gel point: quiescent and shear-induced crystallization, *Polymer* **42**, 9031–9043.

Pooga, M., Land, T., Bartfai, T., Langel, Ü.: 2001, PNA oligomers as tools for specific modulation of gene expression, *Biomol. Eng.* **17**, 183–192.

Rasmussen, S., Chen, L., Nilsson, M., and Abe, S.: 2003, Bridging nonliving and living matter, *Artif. Life* **9**, 269–316.

Sandars, P. G. H.: 2003, A toy model for the generation of homochirality during polymerization, *Orig. Life Evol. Biosph.* **33**, 575–587.

Saito, Y. and Hyuga, H.: 2004, Complete homochirality induced by the nonlinear autocatalysis and recycling, *J. Phys. Soc. Jap.* **73**, 33–35.

Tedeschi, T., Corradini, R., Marchelli, R., Pushl, A., and Nielsen, P. E.: 2002, Racemization of chiral PNAs during solid-phase synthesis: effect of the coupling conditions on enantiomeric purity, *Tetrahedron: Asymmetry* **13**, 1629–1636.

Wattis, J. A. D. and Coveney, P. V.: 1999, The origin of the RNA world: a kinetic model, *J. Phys. Chem. B* **103**, 4231–4250.

Wattis, J. A. D. and Coveney, P. V.: 2004, Symmetry-breaking in chiral polymeri-
    sation, arXiv:physics/0402091.
Woese, C.: 1967, *The Genetic Code*, New York: Harper and Row.